Electrochemistry Communications 82 (2017) 71–74

Contents lists available at ScienceDirect

Electrochemistry Communications

journal homepage: www.elsevier.com/locate/elecom

"Water-in-Salt" electrolyte enabled $LiMn_2O_4/TiS_2$ Lithium-ion batteries

Wei Sun[a,b], Liumin Suo[a], Fei Wang[a], Nico Eidson[a], Chongyin Yang[a], Fudong Han[a], Zhaohui Ma[a], Tao Gao[a], Min Zhu[b], Chunsheng Wang[a,*]

[a] Department of Chemical and Bimolecular Engineering, University of Maryland, College Park, MD 20740, USA
[b] School of Materials Science and Engineering, South China University of Technology, Guangzhou 510641, China

ARTICLE INFO

Keywords:
Aqueous lithium-ion batteries
Anode
TiS_2
"Water-in-Salt" electrolyte

ABSTRACT

High electrochemical reversibility of the TiS_2 anode in "Water-in-Salt" electrolyte (21 m LiTFSI in H_2O) is demonstrated for the first time. The wide electrochemical window and low chemical activity of H_2O in the "Water-in-Salt" electrolyte not only significantly enhanced the electrochemical reversibility of TiS_2 but also effectively suppressed the hydrolysis side reaction in the aqueous electrolyte. Paired with a $LiMn_2O_4$ cathode, the $LiMn_2O_4/TiS_2$ full cell delivers a relatively high discharge voltage of 1.7 V and an energy density of 78 Wh kg^{-1} as well as a satisfactory rate performance.

1. Introduction

The traditional lithium-ion (Li-ion) batteries have been widely used as high energy density power sources for various portable devices. However, the safety concern due to the use of the flammable organic electrolyte solvents has raised much attention in recent years [1–3]. Replacement of organic electrolytes by aqueous electrolytes can allow for intrinsically safe batteries [4–6]. However, the low energy density induced by the narrow thermodynamic stability window of water hinders their future widespread applications [7,8]. Recently, the thermodynamic stability window of water has been significantly extended from 1.5 V to 3.0 V (1.9–4.9 V vs. Li/Li^+) through increasing the salt concentration, which enables more suitable electrode materials and more choices for current collectors in the aqueous battery system [9–17].

Among all the electrode materials used in traditional Li-ion batteries, titanium disulfide (TiS_2) is a well-known intercalation cathode material for the Li-ion battery with a lithium intercalation/deintercalation potential at 2.1 V vs. Li/Li^+ [18,19], which sits well inside of the stability window of the "Water-in-Salt" (WIS) electrolyte. In addition, the TiS_2 also shows a high theoretical specific capacity of 240 mAh g^{-1}, excellent cycling stability, and high electronic/ionic conductivity, making it an attractive anode for the aqueous Li-ion battery (ALIB) in the WIS electrolyte [20–22]. To the best of our knowledge, TiS_2 has never been explored in aqueous electrolytes. It is because the operation potential of TiS_2 is lower than that of the hydrogen evolution (2.6 V vs. Li/Li^+) in the traditional, neutral aqueous electrolytes.

In this work, we investigated the electrochemical performance of TiS_2 anode in the WIS electrolyte (21 mol LiTFSI in 1 kg H_2O, 21 m). The expanded stability window and substantial reduction of water chemical activity not only enable the reversible electrochemical reaction between TiS_2 and Li^+ but also significantly suppress the irreversible parasitic reaction [9,12]. The $LiMn_2O_4/TiS_2$ full cell using commercial $LiMn_2O_4$ as cathode and "Water-in-Salt" as electrolyte shows one of the best electrochemical performances of ALIBs reported to date.

2. Experimental

2.1. Material

Lithium bis(trifluoromethane sulfonyl)imide ($LiN(SO_2CF_3)_2$, LiTFSI) (> 98%) and lithium nitrate ($LiNO_3$) were purchased from Tokyo Chemical Industry and Sigma-Aldrich, respectively. The aqueous "Water-in-Salt" electrolyte was prepared by dissolving 21 mol LiTFSI in 1 kg deionized H_2O (21 m LiTFSI electrolyte). The salt-in-water control electrolytes were made by dissolving 1 m $LiNO_3$ and 1 m LiTFSI in deionized H_2O, respectively. The anode material TiS_2 (Sigma-Aldrich) and cathode material $LiMn_2O_4$ (MTI Corporation) were used as received without further purification.

2.2. Material characterizations

The crystal structure of the samples was studied by powder X-ray diffraction (XRD) using a Cu Kα radiation source on a D8 Advance X-ray diffraction (Bruker AXS, WI, USA) operated at 40 kV and 40 mA. Scanning electron microscope (SEM) was used to investigate the

* Corresponding author.
E-mail address: cswang@umd.edu (C. Wang).

http://dx.doi.org/10.1016/j.elecom.2017.07.016
Received 21 June 2017; Received in revised form 20 July 2017; Accepted 20 July 2017
Available online 22 July 2017
1388-2481/

morphologies of the samples.

2.3. Electrochemical tests

The electrochemical stability windows of 1 m $LiNO_3$, 1 m LiTFSI, and 21 m LiTFSI electrolytes were measured on inert, stainless steel (SS), current collectors by linear sweep voltammetry experiments at a scan rate of 10 mV s^{-1} using an electrochemical workstation (CHI 600E). Both TiS_2 anodes and $LiMn_2O_4$ cathodes were fabricated by compressing active materials, carbon black, and polytetrafluoroethylene (PTFE) at a weight ratio of 8:1:1 on a SS grid. The electrochemical performance of $LiMn_2O_4/TiS_2$ full cell was evaluated using a CR2032-type two-electrode coin cell with glass fiber as the separator. The mass ratio of $LiMn_2O_4$ to TiS_2 was set to be 2:1 by weight to balance the capacities of the anode and cathode. The mass loading of $LiMn_2O_4$ and TiS_2 are about 4.2 and 2.1 mg cm^{-2}, respectively. Lithiation/delithiation behavior of $LiMn_2O_4$ cathodes and TiS_2 anodes in a three-electrode cell and $LiMn_2O_4/TiS_2$ full cell was evaluated by cyclic voltammetry (CV) at a scanning rate of 0.3 mV s^{-1} using the electrochemical workstation. The electrochemical performance of $LiMn_2O_4/TiS_2$ full cells with different electrolytes was evaluated using coin cells using a battery test system (Land CT-2001A). The current density was calculated based on the mass of the anode, and the 1C was defined as 240 mA g^{-1} based on the theoretical specific capacity of TiS_2 (240 mAh g^{-1}). All the electrochemical measurements were performed at room temperature.

3. Results and discussion

The XRD in Fig. 1a reveals that the as-received TiS_2 material has a pure layered crystal structure (JCPDS-15-0853). Additionally, the SEM images of pristine TiS_2 powder in Fig. 1b show that the as-received sample has an irregular shape and its particle size ranged from a few to dozens of micrometers.

Electrochemical stability windows of the different electrolytes were measured in a three-electrode cell using linear sweep voltammetry with SS grid as both working and counter electrodes and the Ag/AgCl as a reference electrode. As labeled in the Fig. 2a, the redox potential range of $LiMn_2O_4$ cathode lies well within the cathode limit of the three electrolytes. However, a small peak at 4.2 V (vs. Li/Li +) was found in 1 m LiTFSI electrolyte. We speculate that this peak may be due to the reaction between the $TFSI^-$ anions and SS current collector when the concentration of $TFSI^-$ anion is low (e.g. 1 m LiTFSI electrolyte), which is similar to the corrosion reaction of an Al current collector in 1 m LiTFSI electrolyte as reported by another research group [15].On the anode side, the redox potential range of TiS_2 sits far below the cathodic limit of the 1 m $LiNO_3$ and 1 m LiTFSI (~2.7 V vs. Li/Li^+) electrolytes, which means the water in the dilute electrolytes was reduced to produce H_2 before the Li^+ intercalation into TiS_2. As the voltage profiles presented in Fig. 2b and c, the $LiMn_2O_4/TiS_2$ full cells in salt-in-water electrolytes (1 m LiTFSI or 1 m $LiNO_3$) exhibited inferior electrochemical performance as expected. The long voltage plateau during the first charge process indicates severe H_2O decomposition. In contrast, the Li-ion intercalation/deintercalation of TiS_2 occurs well above the cathodic limit potential of 1.9 V (vs. Li/Li^+) in the highly-concentrated WIS electrolyte, thus the hydrogen evolution reaction can be effectively suppressed.

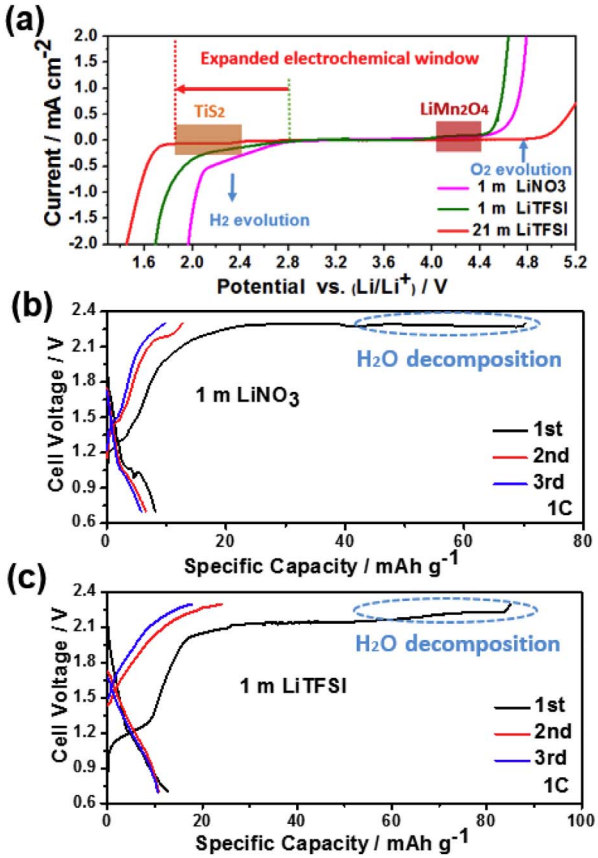

Fig. 2. Electrochemical stability windows of aqueous electrolytes and electrochemical behaviors of electrodes. a. Electrochemical stability window of 1 m $LiNO_3$, 1 m LiTFSI, and 21 m LiTFSI electrolytes as measured on inert current collector (stainless steel grid) using linear sweep voltammetry experiments at a scan rate of 10 mV s^{-1}. The redox potential ranges of TiS_2 and $LiMn_2O_4$ electrodes are also labeled on the graph. b, c. Voltage profiles of full-cell configuration ($LiMn_2O_4/TiS_2$) in (b) 1 m $LiNO_3$, (c) 1 m LiTFSI electrolytes at 1C. The potentials have been converted to Li/Li^+ reference for convenience.

The electrochemical properties of the TiS_2 electrode in WIS

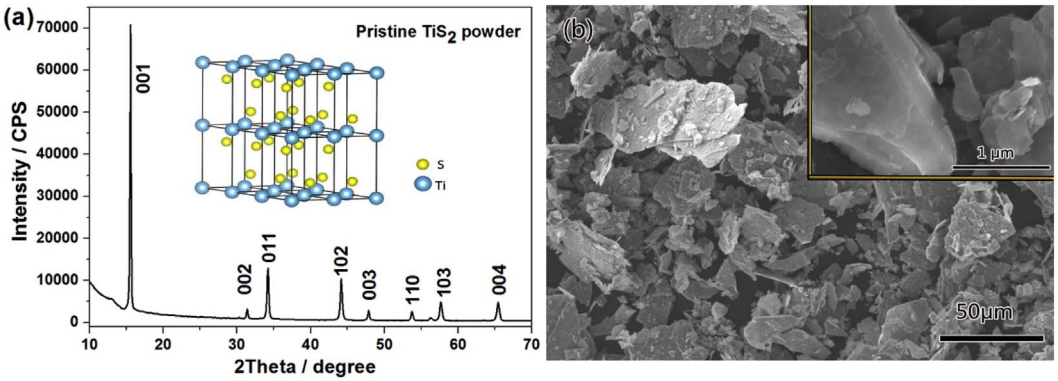

Fig. 1. Structural and morphological characterization of pristine TiS_2 powder. a. X-ray pattern and crystal structure scheme. b. Typical SEM image. The inset of (b) shows a magnified SEM image.

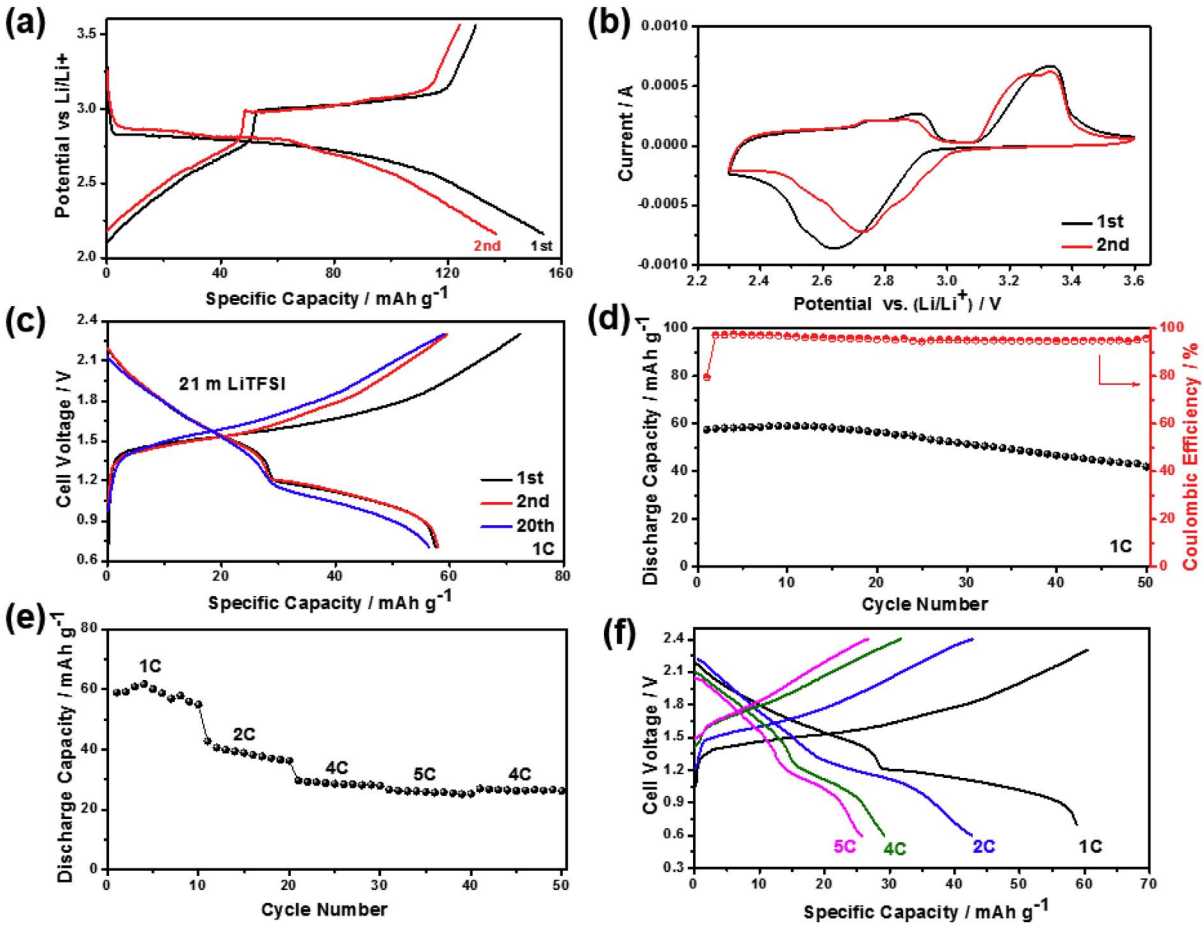

Fig. 3. Electrochemical properties of the TiS_2 electrode and the $LiMn_2O_4/TiS_2$ full cell in WIS electrolyte. a. The galvanostatic charge/discharge behavior of TiS_2 electrode in the 1st and 2nd cycle at 1C. b. Cyclic voltammetry (CV) of TiS_2 electrode in 1st and 2nd cycles at 1 mV s^{-1}. The electrochemical behavior of the TiS_2 electrode was tested in a three-electrode cell using TiS_2 as a working electrode, Ag/AgCl as a reference electrode, and $LiMn_2O_4$ as a counter electrode. c. The galvanostatic charge/discharge of the $LiMn_2O_4/TiS_2$ full cell at 1st, 2nd, and 20th cycles. d. Cycling performance and corresponding voltage profiles of the $LiMn_2O_4/TiS_2$ full cell at a constant current of 1C. e, f. Rate performance and corresponding voltage profiles of the $LiMn_2O_4/TiS_2$ full cell. All the capacity of the $LiMn_2O_4/TiS_2$ full cell shown in Fig. 3 is calculated based on the total electrode masses of $LiMn_2O_4$ and TiS_2.

electrolyte were investigated in a three-electrode cell using TiS_2 as a working electrode, Ag/AgCl as a reference electrode, and $LiMn_2O_4$ as a counter electrode. As shown in the Fig. 3a, the discharge curve of TiS_2 displays a plateau at ~2.8 V followed by a slope at ~2.5 V with a total capacity of ~160 mAh g^{-1} in the first cycle, which is lower than the theoretical capacity (240 mAh g^{-1}), due to the large particle size of the commercial product and high cycling current of 1 C. In addition, the CV of the TiS_2 electrode in WIS electrolyte in Fig. 3b was also consistent with the charge-discharge curves (Fig. 3a). Since the electrochemical window of the WIS electrolyte is wide enough to support the reversible lithiation/delithiation of both the $LiMn_2O_4$ cathode and TiS_2 anode, the $LiMn_2O_4/TiS_2$ full cell was thus assembled. To compensate for the irreversible Li consumption during the solid electrolyte interphase (SEI) formation process on the TiS_2 anode in the first cycle, the cathode/anode mass ratio was set to be 2:1 [13]. As shown in the Fig. 3a, the full-cell shows a highly reversible reaction without an obvious H_2O decomposition plateau. The full cell delivers two stages of voltage (1.7 V and 1.0 V) with a total energy density of 78 Wh kg^{-1} based on the total mass of both cathode and anode.

Fig. 3b shows the cycling performance of the $LiMn_2O_4/TiS_2$ full cell in the WIS electrolyte at the current density of 1C. The full cell displays a discharge capacity of 58 mAh g^{-1} at the first cycle and retained at 43 mAh g^{-1} after 50 cycles, with a capacity retention of 74%. However, we have to note that there still is a slightly irreversible parasitic reaction in the charge/discharge processes, which causes the capacity decay and the relatively low coulombic efficiency below 97% in the subsequent cycles. This irreversible reaction could be suppressed by surface modification like carbon coating. The rate performance of the $LiMn_2O_4/TiS_2$ full cell was further evaluated and shown in Fig. 3c and d. At the 5C rate, the $LiMn_2O_4/TiS_2$ full cell demonstrates a 40% retention of the capacity at 1C.

Fig. 4a shows the X-ray diffraction (XRD) patterns of the TiS_2 electrode in pristine state, after the first charge (lithiation), after the first charge-discharge cycle, and after soaking in the WIS electrolyte for 30 days. As shown in Fig. 4a, the main characteristic peaks of pristine TiS_2 at 16° shift to a lower degree after the first charge due to the intercalation of Li^+. The peak shifts back to around 16° during the following discharge, indicating a highly reversible Li^+ deintercalation. To further confirm the stability of TiS_2 in the WIS electrolyte, the TiS_2 electrode was soaked in the electrolyte for 30 days and then rinsed for the XRD test. The XRD patterns after storage did not show obvious difference from the pristine one, demonstrating the excellent storage stability of TiS_2 electrode in this electrolyte. The morphology change of the TiS_2 electrode after cycling was also examined by the SEM. As shown in Fig. 4b, the TiS_2 particles still were tightly connected with the conductive agent and no evident crack could be observed in the cycled electrode compared with the pristine one. The structural stability also demonstrates the feasibility of using TiS_2 as anode in the WIS electrolyte.

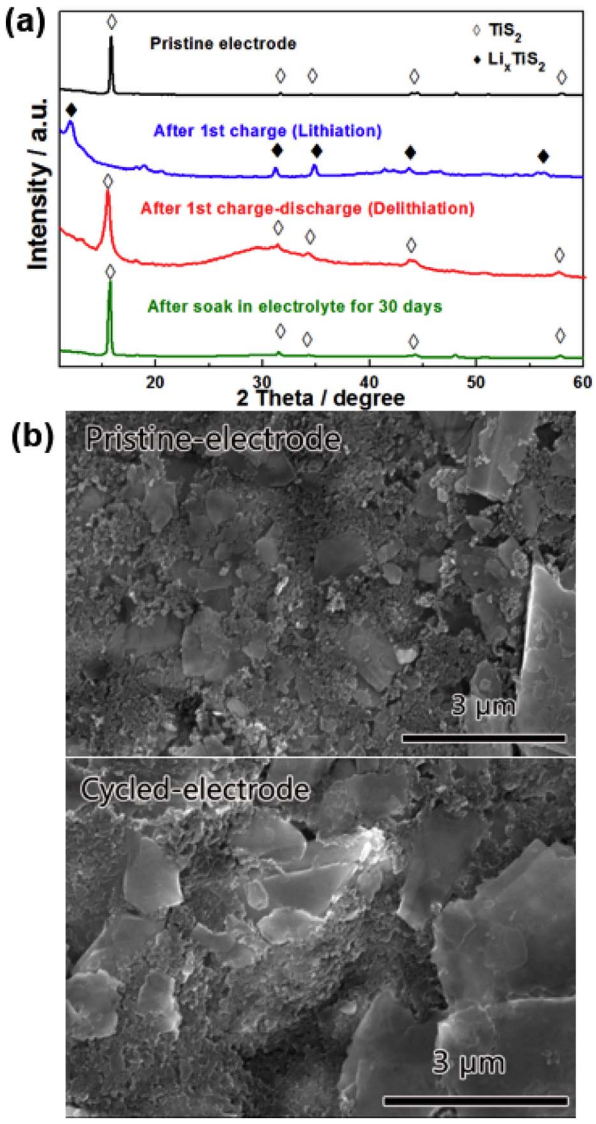

Fig. 4. Post-mortem study of TiS_2 electrode after cycling. a. X-ray diffraction patterns of TiS_2 electrodes: pristine (black), after first charge (blue), after first charge-discharge (red), and after soaked in the WIS electrolyte for 30 days (green). b. SEM images of TiS_2 electrodes before and after 20 cycles in the WIS electrolyte. (For interpretation of the references to colour in this figure legend, the reader is referred to the web version of this article.)

4. Conclusion

In summary, we demonstrated that the TiS_2 electrode material in liquid organic electrolyte Li-ion batteries can be utilized as an anode in WIS electrolyte Li-ion batteries. Paired with a $LiMn_2O_4$ cathode, the $LiMn_2O_4/TiS_2$ full cell delivered a high discharge voltage of 1.7 V and energy density of 78 Wh kg^{-1}. These results reveal a promising future for exploring more anode materials for the intrinsically safe aqueous batteries. Furthermore, this work also raises the possibility of using metal sulfides in the aqueous system.

Conflict of interest

The authors declare no conflict of interests.

Acknowledgments

The authors acknowledge the financial support of DOE ARPA-E (DEAR0000389) and the technical support of the NanoCenter at the University of Maryland. Wei Sun was supported by a fellowship from China Scholarship Council (201506150044).

References

[1] G. Wang, L. Fu, N. Zhao, L. Yang, Y. Wu, H. Wu, An aqueous rechargeable lithium battery with good cycling performance, Angew. Chem. Int. Ed. Eng. 46 (2007) 295–297.
[2] J.Y. Luo, W.J. Cui, P. He, Y.Y. Xia, Raising the cycling stability of aqueous lithium-ion batteries by eliminating oxygen in the electrolyte, Nat. Chem. 2 (2010) 760–765.
[3] C. Wessells, R. Ruffo, R.A. Huggins, Y. Cui, Investigations of the Electrochemical Stability of Aqueous electrolytes for lithium battery applications, Electrochem. Solid-State Lett. 13 (2010) A59–A61.
[4] W. Tang, Y. Zhu, Y. Hou, L. Liu, Y. Wu, K.P. Loh, H. Zhang, K. Zhu, Aqueous re-chargeable lithium batteries as an energy storage system of superfast charging, Energy Environ. Sci. 6 (2013) 2093–2104.
[5] W. Li, J.R. Dahn, D.S. Wainwright, Rechargeable lithium batteries with aqueous electrolytes, Science 264 (1994) 1115–1118.
[6] W. Li, J.R. Dahn, Lithium-ion cells with aqueous electrolytes, J. Electrochem. Soc. 142 (1995) 1742–1746.
[7] H. Manjunatha, G.S. Suresh, T.V. Venkatesha, Electrode materials for aqueous re-chargeable lithium batteries, Electrochem. Solid-State Lett. 15 (2010) 431–445.
[8] J. Zhao, K.K. Sonigara, J. Li, J. Zhang, B. Chen, J. Zhang, S.S. Soni, X. Zhou, G. Cui, L. Chen, A smart flexible zinc battery with thermoreversible hydrogel electrolyte, Angew. Chem. Int. Ed. Eng. 129 (2017) 7979–7983.
[9] L. Suo, O. Borodin, T. Gao, M. Olguin, J. Ho, X. Fan, C. Luo, C. Wang, K. Xu, "Water-in-salt" electrolyte enables high-voltage aqueous lithium-ion chemistries, Science 350 (2015) 938–943.
[10] F. Wang, L. Suo, Y. Liang, C. Yang, F. Han, T. Gao, W. Sun, C. Wang, Spinel LiNi0. 5Mn1. 5O4 cathode for high-energy aqueous lithium-ion batteries, Adv. Energy Mater. (2016) 1600922.
[11] F. Wang, Y. Lin, L. Suo, X. Fan, T. Gao, C. Yang, F. Han, Y. Qi, K. Xu, C. Wang, Stabilizing high voltage LiCoO 2 cathode in aqueous electrolyte with interphase-forming additive, Energy Environ. Sci. 9 (2016) 3666–3673.
[12] L. Suo, F. Han, X. Fan, H. Liu, K. Xu, C. Wang, "Water-in-Salt" electrolytes enable green and safe Li-ion batteries for large scale electric energy storage applications, J. Mater. Chem. A 4 (2016) 6639–6644.
[13] L. Suo, O. Borodin, W. Sun, X. Fan, C. Yang, F. Wang, T. Gao, Z. Ma, M. Schroeder, A. von Cresce, Advanced high-voltage aqueous lithium-ion battery enabled by "Water-in-Bisalt" electrolyte, Angew. Chem. Int. Ed. Eng. 128 (2016) 7252–7257.
[14] J. Zhao, Y. Li, X. Peng, S. Dong, J. Ma, G. Cui, L. Chen, High-voltage Zn/LiMn 0.8 Fe 0.2 PO 4 aqueous rechargeable battery by virtue of "water-in-salt" electrolyte, Electrochem. Commun. 69 (2016) 6–10.
[15] R.-S. Kühnel, D. Reber, A. Remhof, R. Figi, D. Bleiner, C. Battaglia, "Water-in-salt" electrolytes enable the use of cost-effective aluminum current collectors for aqueous high-voltage batteries, Chem. Commun. 52 (2016) 10435–10438.
[16] L. Coustan, G. Shul, D. Bélanger, Electrochemical behavior of platinum, gold and glassy carbon electrodes in water-in-salt electrolyte, Electrochem. Commun. 77 (2017) 89–92.
[17] A. Gambou-Bosca, D. Bélanger, Electrochemical characterization of MnO2-based composite in the presence of salt-in-water and water-in-salt electrolytes as electrode for electrochemical capacitors, J. Power Sources 326 (2016) 595–603.
[18] R. Elazari, G. Salitra, G. Gershinsky, A. Garsuch, A. Panchenko, D. Aurbach, Li Ion cells comprising lithiated columnar silicon film anodes, TiS2 cathodes and fluor-oethyene carbonate (FEC) as a critically important component, J. Electrochem. Soc. 159 (2012) A1440–A1445.
[19] M. Winter, J.O. Besenhard, M.E. Spahr, P. Novák, Insertion electrode materials for rechargeable lithium batteries, Adv. Mater. 10 (1998) 725–763.
[20] M.S. Whittingham, Lithium batteries and cathode materials, Chem. Rev. 104 (2004) 4271–4302.
[21] J.E. Trevey, C.R. Stoldt, S.-H. Lee, High power nanocomposite TiS2 cathodes for all-solid-state lithium batteries, J. Electrochem. Soc. 158 (2011) A1282–A1289.
[22] R. Winter, P. Heitjans, Li + diffusion and its structural basis in the nanocrystalline and amorphous forms of two-dimensionally ion-conducting LixTiS2, J. Phys. Chem. B 105 (2001) 6108–6115.